

## Characterisation of the Features of Seat-belt Systems Based on the Analysis of Large Crash Databases

Manuel Valdano, Jesús R. Jiménez-Octavio, Bengt Pipkorn, Francisco J. López-Valdés

**Abstract** The goal of this study was to develop a method to analyse the seat-belt force-time history measurements obtained from laboratory crash tests to characterise the pre-tensioner and load-limiting features. The study also aimed to describe how these characteristics have changed over the past 40 years using NHTSA's crash test database. The method was used to identify the pre-tensioner time-to-fire (TTF) and force level, and load-limiter force by analysing the shape of the force-time history curves measured at the lap and shoulder belts in laboratory crash tests. The method was applied to the full-width frontal crash tests at 56 km/h of the New Car Assessment Program (NCAP), gathered from the NHTSA vehicle crash test database from the last 40 years. The algorithm's accuracy in identifying the presence of a pre-tensioner and load limiter was 90% and 89%, respectively. The adoption of both devices started in the mid-1990s, and they were widely adopted in most tested vehicles by 2005. The study provides ranges for the TTF and force of the pre-tensioner and load-limiter force for different configurations of the seat-belt system. The algorithm was successfully developed and validated, making it useful for future injury risk studies.

**Keywords** Seat-belt, pre-tensioner, load limiter, characterisation, frontal crashes.

### I. INTRODUCTION

In 2020, the number of motor vehicle-related fatalities in the United States was 38,824, according to the last available data from the Fatality Analysis Reporting System (FARS) [1], which resulted in a 6.8% increase with respect to 2019. As for non-fatal injuries, the National Highway Traffic Safety Administration (NHTSA) estimated that around 4.5 million people were injured in motor vehicle crashes in the United States in 2019 [2]. Of these injuries, 806,000 involved severe injuries (AIS3+), according to the Abbreviated Injury Scale [3].

Experimental studies using Post-Mortem Human Subjects (PMHS) and Anthropomorphic Test Devices (ATD) and also studies using computational human body models (HBM) have shown that seat-belt systems incorporating pre-tensioners and force-limiting features were effective in the prevention of thoracic injuries [4-8]. In parallel, epidemiological studies have suggested that even if experimental studies (involving physical or computational testing) might be relevant to design and assess the nominal effect of more advanced restraint systems, it is only when the systems are evaluated using real-world injury data that its true effectiveness can be estimated [9].

While NASS CDS has been an essential source of data for these epidemiological evaluations, given the detailed information collected in the system, the aforementioned characteristics of advanced seat belts are not included in the database, making it difficult to assess their effect using real-world data. Furthermore, the actual characteristics of these devices are not publicly available as vehicle manufacturers do not share them. The assessment of the real-world effectiveness of advanced restraint systems would require a database that includes a description of the seat-belt pre-tensioners and load limiters installed in the vehicles.

The U.S. Department of Transportation's National Highway Traffic Safety Administration (NHTSA) provides information to consumers on the crashworthiness performance of vehicles through the New Car Assessment Program (NCAP). The NCAP program uses various crash conditions, such as front and side-impact crashes and rollover resistance, to test the crashworthiness of vehicles. The data generated from these tests are shared with consumers through a user-friendly five-star rating system, while the technical data are available via the NHTSA's research testing database [10]. This database contains detailed reports, videos, pictures and time history measurements from the tests, which can be utilised to identify the features of the restraint system.

Thus, this study aimed to develop and validate an automatic method to characterise the seat-belt pre-tensioner and load limiter characteristics based on force time history measurements recorded in NHTSA's crash tests. Once developed, the method was applied to produce a descriptive analysis of how seat-belt characteristics have evolved over the last 40 years.

## II. METHODS

### **Data Source**

Data were gathered from NHTSA's vehicle crash test database from 1980 onwards. Crash tests were filtered to retain the 56 km/h full-width frontal tests carried out under the NCAP program. The metadata and ISO-MME files of these crash tests were downloaded from the NHTSA webpage [10] to be used to develop automatic characterisation algorithms, to assess their performance characterising the seat belts, and to describe the characteristics of the restraint systems used in the tested vehicles.

ISO-MME files were used to extract the force-time history curve measured at the driver's and passenger's lap and shoulder belts. The channel code and comments in these files were used to identify where the force-time history curve was measured in the tests. Instrumentation metadata and the comment section of the ISO-MME files were used to look for keywords suggesting questionable and lost data or channel failure, and these readings were then disregarded. Using a linear interpolation method, the retained seat-belt force signals were then re-sampled to 10kHz.

### **Validation Subset**

From the group of downloaded seat-belt force curves, a subset of 60% of them were chosen to serve as the validation subset of the automatic algorithms to be developed later. The curves in the validation subset were inspected manually by a group of 9 people to determine the characteristics of the restraint systems in the validation subset. These individuals were finalizing the second year of the Master's program on Mobility and Safety at Universidad Pontificia Comillas, and all of them had completed several courses on injury biomechanics, restraint systems and crashworthiness. In addition, specific instructions about the procedure were provided to the group, and assistance from the authors of this work was given when needed. The instructions defined what characteristics and how they should be classified according to the time-history signal of the seat-belt forces. These instructions are shown in the Appendix.

As the actual configuration of the pre-tensioning and load-limiting devices used in vehicles was not available, after completion of the aforementioned manual inspection, the identified values were reviewed by the authors to prevent any misclassifications. These values were then used to tune the identification algorithms and to assess their performance in classifying the seat-belt features.

### **Pre-tensioner Characteristics: Time-to-fire and Peak Force**

An algorithm was developed to identify three characteristics of the pre-tensioner: whether a pre-tensioner was present; the magnitude of the pre-tensioner force; and TTF. The lap- and shoulder-belt force-time history curves were analysed independently to identify these characteristics in each portion of the seat-belt system. This analysis was restricted to the first 30 ms of the crash phase. A CFC 180 filter was applied to the signals to eliminate undesired noise.

From the time history curve of the corresponding seat-belt force, a sliding time window was applied to each signal to measure the peak-to-peak (PTP) force difference inside the time considered by the window. The application of this technique resulted in a second curve, which showed the PTP difference in the time window, as illustrated in Figure 1. In the figure, the time window analysed is shown as a shadowed red rectangle in the original force-time history curve. The PTP force in this period was plotted at the time represented by the red line in the resultant curve on the right subfigure. A negative value was obtained if the highest value was observed before the lowest value. The widths of the sliding windows were between 0.5 and 5.0 ms, with increments of 0.5 ms. The sliding window width was selected by maximising the pre-tensioner identification performance. The criteria for selecting the sliding window width will be explained in detail later in this manuscript. The PTP force-time history curve was used to get the maximum value and time of the peak.

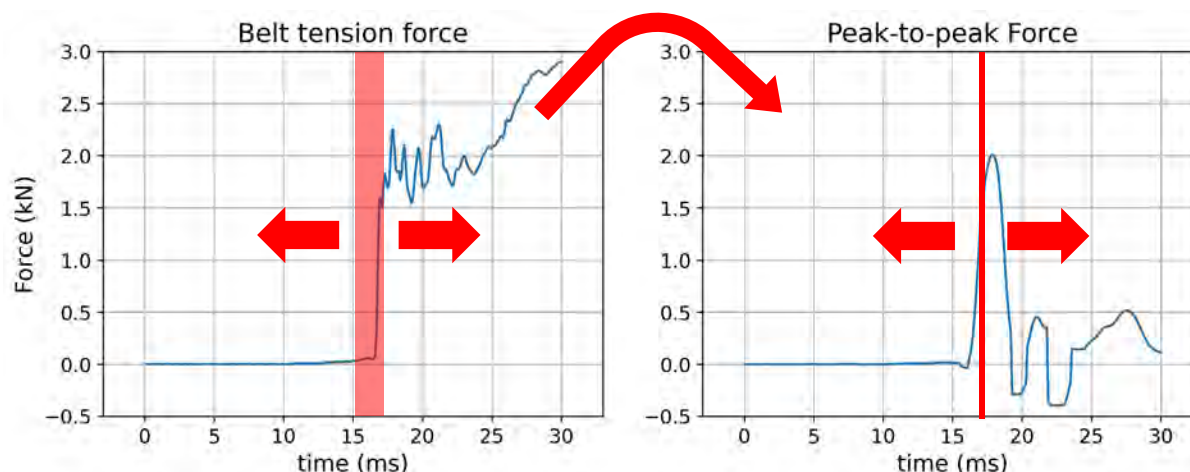


Fig. 1. In red, an example of the sliding window applied to the first 30 ms of a force-time history curve. The plot on the left side shows the original force-time history curve, and the plot on the right side shows the result of applying the sliding window.

A binary classificatory algorithm was then used to classify the systems into two basic categories: restraint systems with and without a pre-tensioner. For this algorithm, the definition of a threshold was necessary, which was used to classify those curves with a maximum value higher than the threshold as a restraint system with a pre-tensioner device in that location. The force-time history curves in the validation subset were used to find the best threshold for each sliding window width.

Various metrics, such as recall, precision, accuracy and the F1-score, were utilised to evaluate the effectiveness of the aforementioned binary classification algorithm. In this study, we defined the presence of a pre-tensioner as a positive case. Recall [11], also known as sensitivity, is the proportion of true positive cases to total positives (i.e. cases with a pre-tensioner that were correctly classified as such by the algorithm over the total number of seat belts with pre-tensioners). Precision [11], or confidence, is the proportion of correctly classified positive cases among all predicted positive cases. Accuracy [12] measures the proportion of all positive or negative cases that the algorithm correctly classified. The F1-score [13] measures the algorithm's overall performance, considering both precision and recall. This score is the harmonic mean of precision and recall, providing a single metric that balances these two measures and is calculated with the following equation:

$$F1\text{-score} = \frac{2 \text{ Recall Precision}}{\text{Recall} + \text{Precision}}, \quad (1)$$

The F1-score was maximised for each sliding window to define the threshold force for detecting a pre-tensioner. This metric was different for each sliding window. The optimal window width and the force threshold were selected to maximise the F1-score across all window widths.

After classifying the seat-belt curves between those without a pre-tensioner and those with a pre-tensioner, the TTF and the force of the pre-tensioner device were determined for the curves included in the second group. A similar process as above was used to identify these parameters but, in this process, the criterion used to identify the TTF and the pre-tensioning force in the data was the minimisation of the means absolute error (MAE) between the algorithm and the validation subset.

Note that as the criteria used for choosing the optimal sliding window width were different depending on the characteristic under study, three different widths were obtained as the optimal ones.

The location of a pre-tensioner can be at the retractor, buckle or anchor plate, and multiple pre-tensioner devices could be simultaneously used for a vehicle occupant. Although the algorithm determines if a pre-tensioning force was observed at the lap or shoulder belt, the actual location of the pre-tensioning device was not determined. Thus, the results are shown in terms of the belt section where a sudden increase of the tension force (i.e., a pre-tension) was observed, which could be either the lap belt, shoulder belt or both.

### **Load Limiter Characteristics**

A second algorithm was developed to detect and characterise load-limiting forces in shoulder-belt force-time history curves. This process was divided into two phases: first, the shape of the force-time history curve was characterised; second, the load-limiting device characteristics were extracted from the previous step.

Previous to the application of the algorithm, the curves were filtered with a CFC 180. After filtering, the curves were re-sampled using the Visvalingam-Whyatt algorithm [14] to obtain a similar shape curve with fewer points, which were not evenly distributed in time. The simplified force-time history curve points were used to obtain groups according to the point distance in the force and time axes, and these points were grouped to obtain the load-limiting force levels. The outcome of this process resulted in three categories: no force limiting in the restraint system; a single-stage force limiting feature in the seat belt (when only one group of points maintaining similar distance between them was found); or a double-stage force limiting seat belt (when two groups of points with similar distance were identified).

Specifically, the requirements so that a group of points was considered to have a similar distance were the following:

- The PTP force between the group points must be smaller than 1.4 kN.
- The group points must be obtained from a continuous time series, i.e. all points from the simplified force-time history curve between the minimum and maximum time of the group must belong to the group.
- The average force of the group points must be higher than 1.5 kN.
- The duration of the group must be longer than 15 ms.

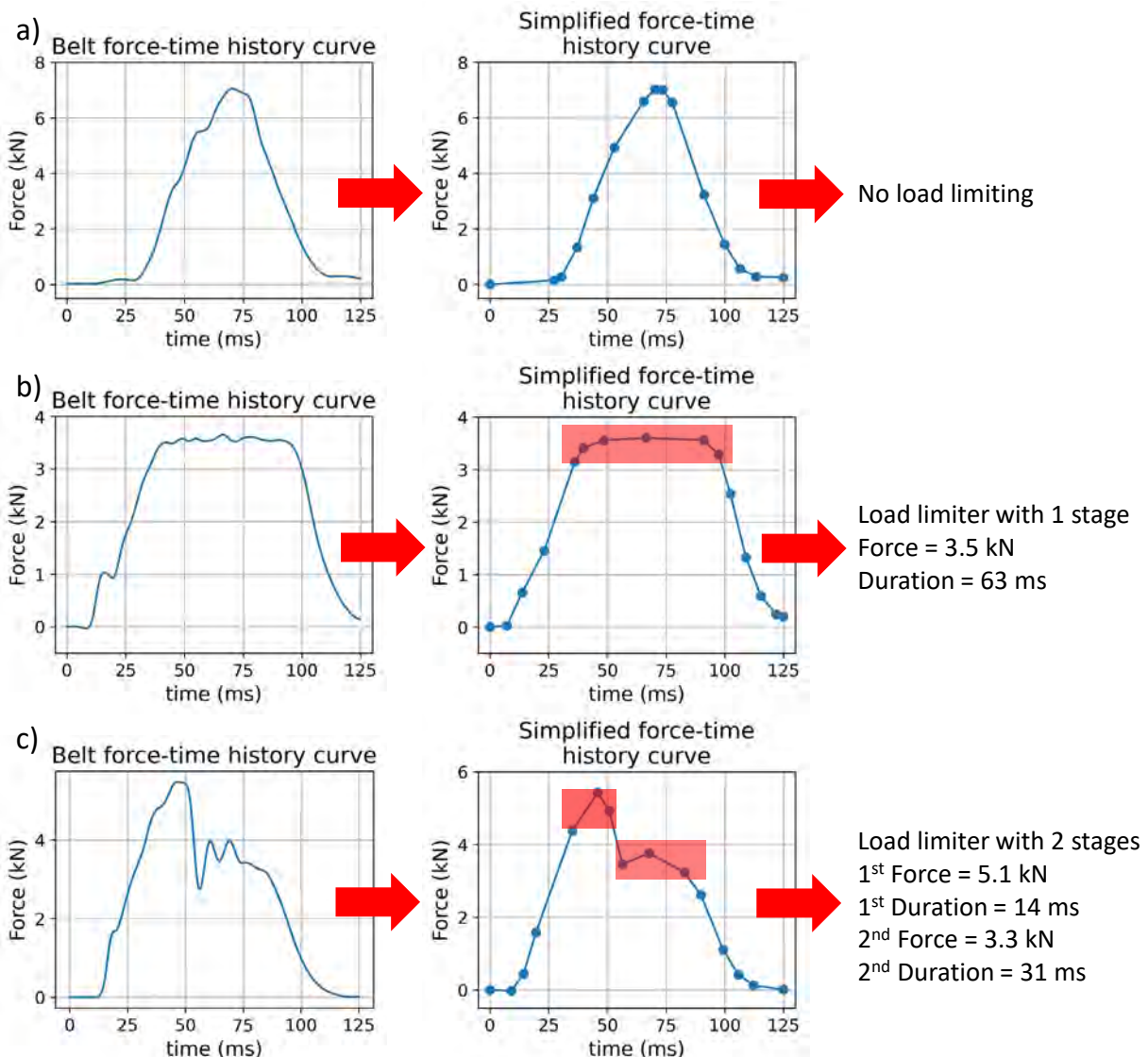


Fig. 2. Example of applying the load-limiting characteristics identification algorithm to cases with no load-limiting device and single and double stage load-limiting device.

After the application of the above conditions, it was noted that the algorithm had difficulties identifying the first load-limiting force in restraint systems with double load-limiting levels. However, it correctly identified the second stage of load limiting. Thus, a time-series K-means clustering method was used to identify, based on their shape, which of the original curves could be associated with a double-stage load-limiting seat belt. The clustering metric used to measure the distance between the time series was the dynamic time warping (DTW) distance. The

cluster corresponding to the double-stage load-limiting seat belts was then used to enhance the predictions of the first stage of load limiting.

Then, a new method was developed to characterise the seat-belt systems that were classified into the cluster associated with double-stage load-limiting seat belts. The requirements to identify the load limiting stages were obtained by applying a genetic optimisation algorithm. The goal of algorithm was to maximize the F1-score in the identification of the load limiting characteristics. The algorithm found the optimal set of values (requirements) for a set of performance characteristics of the load limiting seat belt that achieved this goal. The genetic algorithm required 150 generations with a population of 30 combinations of values to find the following combination that maximised the F1-score:

- The PTP force between the group points must be smaller than 0.79 kN.
- The group points must be obtained from a continuous time series, i.e. all points from the simplified force-time history curve between the minimum and maximum time of the group must belong to the group.
- The average force of the group points must be higher than 1.36 kN.
- The duration of the group must be longer than 5.45 ms.

With the previous variables, it was noted that the algorithm did not perform optimally for some of the seat belts in the sample. These were associated with two specific cases: first, cases in which the algorithm identified the section of the curve right after the firing of the pre-tensioner as a load-limiting stage; and second, cases in which a stable seat-belt force during the rebound of the occupant was identified again as a load limiting stage. The first issue was solved by discarding potential load limiting stages starting earlier than 5 ms after the pre-tensioner TTF. The second one was avoided by filtering out those cases in which the second load limiting stage started later than  $t=75$  ms.

The above method is summarised in Figure 2, which shows examples of the identification of load-limiting characteristics. Subfigure “a” shows an example of a force-time history curve with no load-limiting device. The first figure shows the filtered force-time history curve, followed by the result of the simplification algorithm. No load-limiting device was found for this example, as no group fulfilled the abovementioned requirements. Subfigure “b” shows an example of a force-time history curve with a 1-stage load-limiting device. The simplified force-time history curve shows a constant force of around 3.5 kN. The algorithm identified this load-limiting force, represented in the red shaded area. Subfigure “c” shows an example of a force-time history curve with a two-stage load-limiting device. The simplified force-time history curve shows two stages of the load-limiting device. The algorithm identified the first and second stage, shown as the red-shaded area, with a constant force around 5.1 kN and 3.3 kN, respectively.

The performance of the load limiter identification algorithm was also measured by using recall, precision, accuracy, and F1-score.

### ***Description of the evolution of restraint systems***

A descriptive analysis was performed of how the characteristics of pre-tensioner and load-limiting devices have changed for the vehicles from the last 40 years used at the NCAP full-barrier crash tests. These characteristics were identified using the above-explained algorithms. The descriptive analysis of these devices included the following distributions: percentage of adoption year-by-year of advanced seat-belt devices, description of force and TTF used in pre-tensioner devices, and description of forces used in load-limiting devices.

## **III. RESULTS**

### ***Data Source***

The information from 1,318 analysed crash tests was downloaded from the NHTSA webpage. The resulting number of force-time history curves examined was 5,138, obtained after discarding those curves in which errors in the measurements were identified. The retained curves corresponded to 1,300 and 1,317 force vs. time curves measured at the shoulder and lap belt of the driver position, and 1,237 and 1,284 force vs. time curves measured at the shoulder and lap belt of the front-seat passenger. Figure 3 shows a bar plot with the number of force-time history curves year-by-year used in this study. Each bar is divided into four colours, which shows the location where the force-time history curve was measured. The number of curves oscillated around 150 per year for the period 1982–2002. The lowest number was found for 2003, followed by a rise in the number of curves by year. This number hit two peaks in 2006 and 2012, slowly decreasing afterwards.

Out of the total 5,138 curves, 3,081 force vs time curves were manually labelled by the mentioned group of 9 individuals to describe the pre-tensioner and load-limiting devices. These curves were distributed evenly across the initial categories found in the data: driver seat-belt curves (815 and 740 measured at the shoulder and lap belt, respectively) and front-seat passenger seat-belt curves (805 and 721 measured at the shoulder and lap belt, respectively). The manually labelled curves were used as the validation subset for the results predicted by the algorithms.

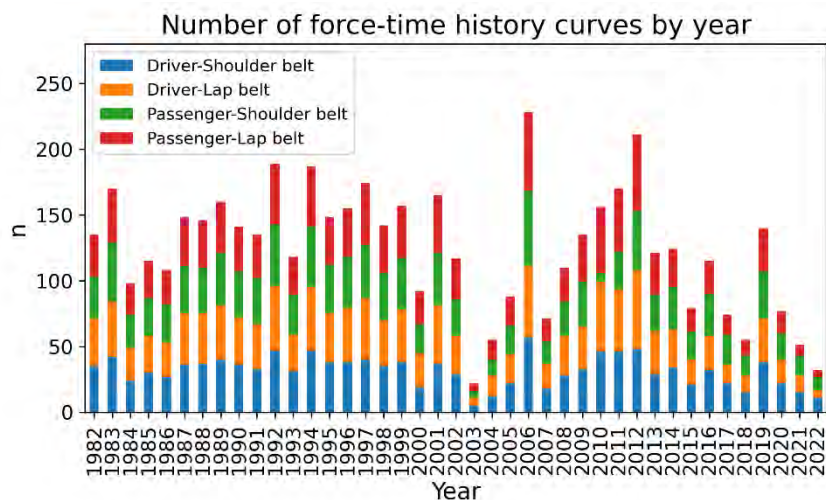


Fig. 3. Number of force-time history curves per year at different vehicle locations.

**Pre-tensioner Time-to-fire and Force Identification**

An algorithm was developed to identify three seat-belt force-time history curve characteristics: whether there was a pre-tensioner incorporated in the seat belt; the pre-tensioning force level; and TTF.

Three different sliding window widths were selected to predict the three characteristics under study. Figure 4 shows the F1-scores and mean absolute error (MAE) used to choose the optimal window widths. Subfigure “a” shows the threshold force and the resulting F1-score for predicting a pre-tensioner presence as a function of the window width. The maximum performance was obtained for a window width of 1 ms and a threshold of 0.51 kN (corresponding to the maximum F1-score). This method obtained a recall, precision, accuracy and F1-score of 95.0%, 89.7%, 95.5% and 92.3%, respectively. Subfigure “b” shows the MAE obtained in the identification of the pre-tensioner (PT) force and time-to-fire (TTF). The minimum MAE for the PT force was obtained using 4 ms as sliding window width, which resulted in an error of 0.17 kN. The minimum MAE for the PT TTF was obtained using 0.5 ms as sliding window width, which resulted in a MAE of 1.09 ms.

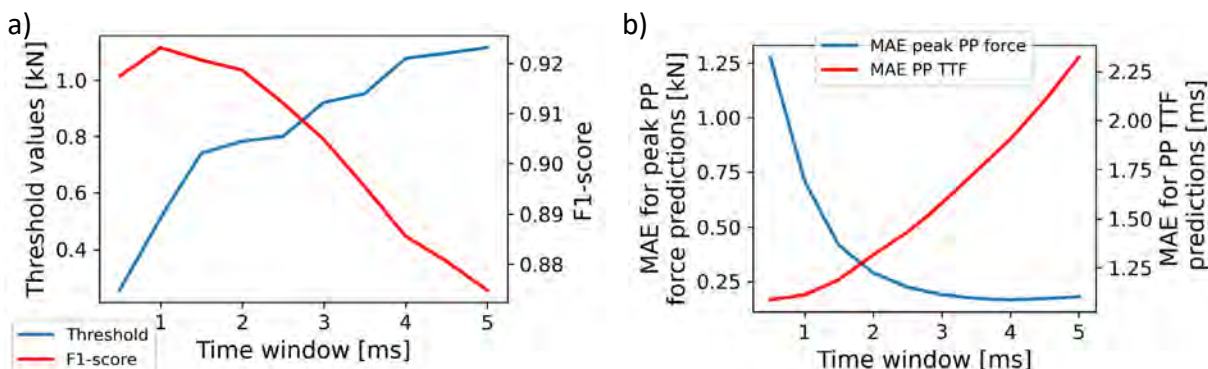


Fig. 4. Performance of the algorithm to characterise the pre-tensioner. a) F1-score, in red, for different sliding window widths and their respective force thresholds, in blue. b) MAE by applying different sliding window widths for the identification of the PT force in blue and PT TTF in red.

**Load Limiter Identification**

Figure 5 shows the results obtained after applying the clustering algorithm to the original data. These clusters were obtained with 20% of the data. The elbow method was used to select the optimum number of clusters, resulting in seven clusters, as shown in the Figure.

The first cluster demonstrated a sustained force over time, suggesting a load-limiting device with one stage. The second and third clusters exhibited a similar shape but did not clearly show the use or not use of a load-limiting device. The fourth cluster showed a first peak followed by a plateau, resembling a load-limiting device with two stages. The fifth and sixth clusters showed data loss due to measurement errors, while the seventh cluster exhibited a peak force of around 110 ms. Therefore, the seat-belt force vs time curves included in the last three clusters were not further included in the analyses. It should be noted that the force-time history curves that were classified within the fourth cluster were identified as potential restraint systems featuring a double-stage load-limiting device and used to enhance the prediction of the algorithm as described in the Methods section, above.

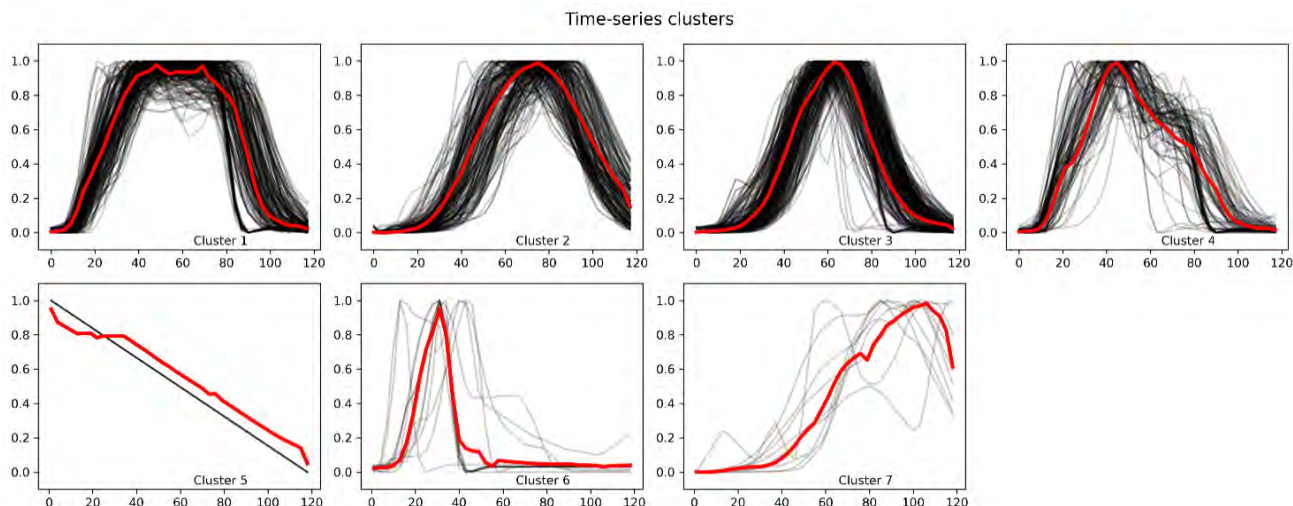


Fig. 5. Cluster centres that were obtained by applying the k-means clustering algorithm in red, and some of the force-time history curves that were identified as part of such clusters in grey.

The application of the classifying algorithm on the original data resulted in three categories: seat belts without load limiting; seat belts incorporating a single-stage load limiting characteristic; and seat belts incorporating a double-stage force limiter. Table I shows the results of the accuracy, F1-score, precision, and recall obtained after comparing the predictions given by the algorithm and the data manually identified in the validation set.

TABLE I  
DETECTION PERFORMANCE OF LOAD-LIMITING DEVICES

	Accuracy	F1-score	Precision	Recall
Presence of a load-limiting feature	0.891	0.898	0.941	0.859
Double-stage load-limiting feature	0.933	0.765	0.872	0.681

The algorithms used to identify and quantify the force-limiting characteristics of seat belts performed slightly worse than those used in analysing the seat-belt pre-tensioners. It should be noted that 75% of the miscategorised cases belonged to vehicles manufactured between 1980 and 2005. Furthermore, 57% of these miscategorised cases corresponded to vehicles manufactured before 1995.

The MAE of the prediction of the load-limiter force was assessed when the use of a load-limiting device was correctly detected. If a double-stage load-limiting device was detected, only the first stage of the load-limiting device was used for the assessment. The MAE for this prediction was 0.23 kN. If a double-stage load-limiting device was detected, the MAE was calculated using the force of the second stage. In this case the MAE was 0.16 kN.

**Description of the Evolution of Restraint Systems**

Force-time history curves were analysed from vehicles over the last 40 years, which were tested in the NCAP full-barrier crash tests. Specifically, a total of 5,138 force-time history curves were studied from 1,355 vehicles to identify the characteristics of pre-tensioner and load-limiting devices.

Figure 6 shows the adoption of pre-tensioner devices for restraint systems used for the driver and passenger. Furthermore, this analysis considered if the pre-tension was observed for the lap or shoulder belt. The red and orange lines show the adoption of these devices in the shoulder belt for the driver and passenger, respectively.

The adoption of these devices was lower than 20% for vehicles tested before 1995 and gradually incremented afterwards. Pre-tensioners for the shoulder belt were used in more than 80% of the vehicles tested after 2004, and this level has been maintained up to the present. The adoption of lap-belt pre-tensioners has been slower, and began after 2002. Adoption levels between 50% and 80% have been found for 2015 onwards. Similar adoption levels have been found for these devices for the driver and front-seat passenger positions.

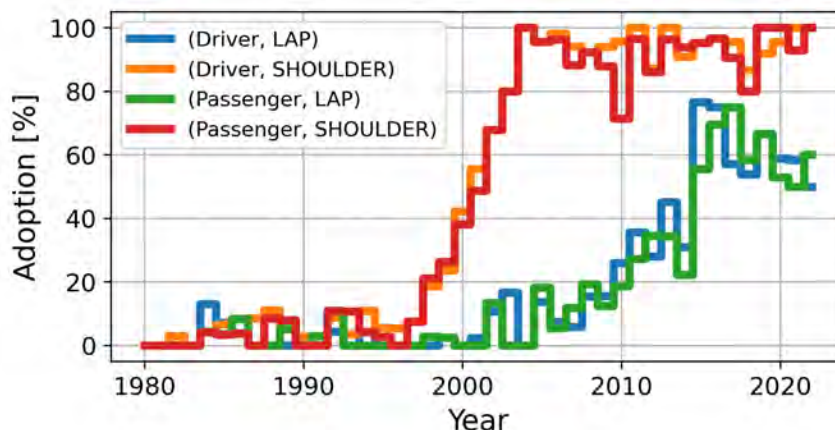


Fig. 6. Adoption of pre-tensioners for different vehicle locations.

Figure 7 shows the mean forces and TTFs used in the pre-tensioner devices. Subfigure “a” shows the mean pre-tensioner force at the lap and shoulder belt in vehicles from 1996 onwards. The forces used in pre-tensioner devices for the shoulder belt have maintained similar values in the time analysed, ranging from 1.5 to 2.0 kN approximately. In contrast, forces used in pre-tensioners for the lap belt have increased from 1.0 to 2.5 kN over the last 20 years. Subfigure “b” shows the mean pre-tensioner TTF at the lap and shoulder belt. Similar values have been identified for these devices in the analysed period, ranging from 15 to 20 ms. However, a small difference in the mean TTF was observed for the lap- and shoulder-belt pre-tensioners from 2010 to 2022. Specifically, the TTF for the lap-belt pre-tensioner was slightly later than that for the shoulder-belt pre-tensioner, with a difference of approximately 2 ms.

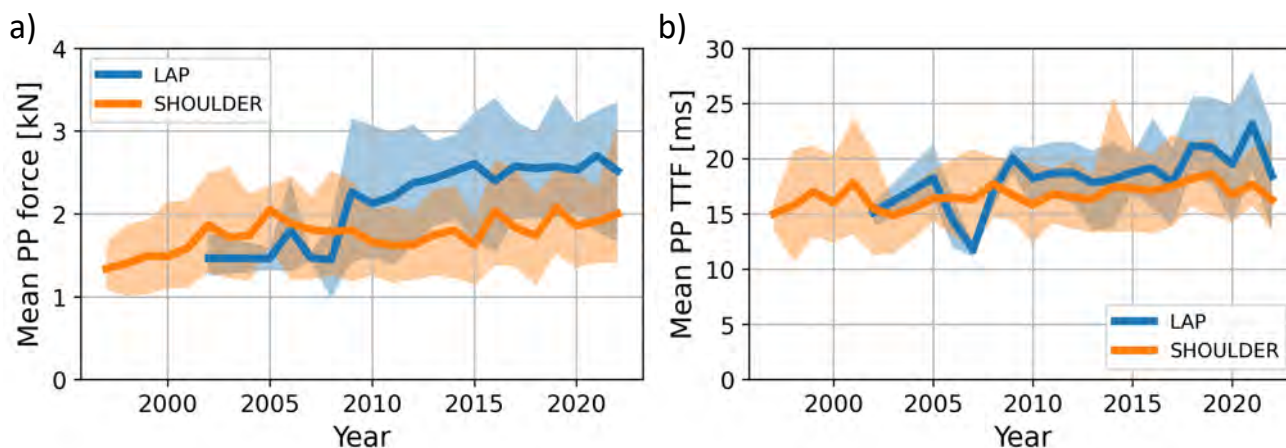


Fig. 7. Mean pre-tensioner (PP) force (subfigure a) and TTF (subfigure b) at the lap and shoulder belt. The shadowed area shows the range between the 10<sup>th</sup> and 90<sup>th</sup> percentiles of the data observed by year.

Figure 8 shows the adoption of load-limiting devices for restraint systems used for the driver and passenger. The red and orange lines show the adoption of these devices for the driver and passenger, respectively. The adoption of these devices was below 20% for vehicles tested before 1998 and gradually incremented afterwards. Load-limiting devices were present in over 80% of tested vehicles after 2003. Similar adoption levels have been observed for driver and passenger restraint systems.

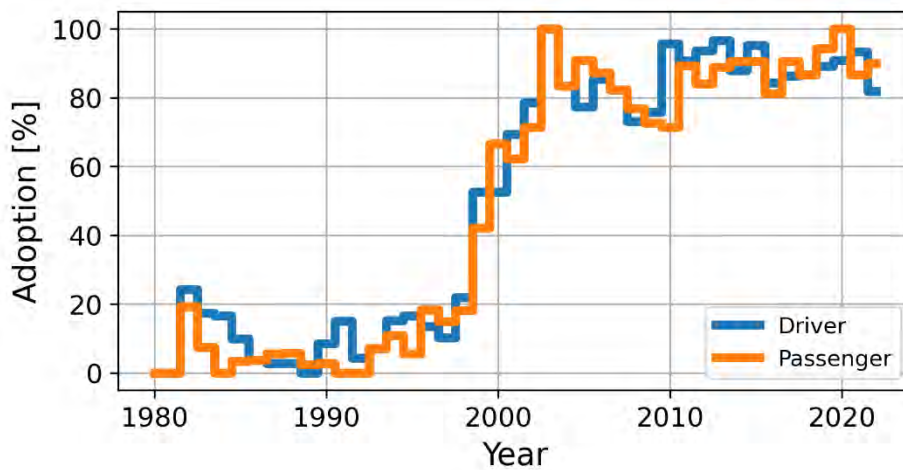


Fig. 8. Adoption of load-limiter devices for the driver and front-seat passenger.

Figure 9 shows the mean forces used in the load-limiting devices in vehicles from 1996 onwards. Forces used in load-limiting devices have decreased in the time analysed, starting at 5 kN and finishing at the range between 3 and 4 kN. This trend was observed for devices used at both driver and front-seat passenger positions. A difference in the mean force was observed for load-limiting devices used for the driver and passenger positions after 2010. A mean 0.6 kN higher force was observed for load-limiting devices at the driver position than for devices at the passenger position.

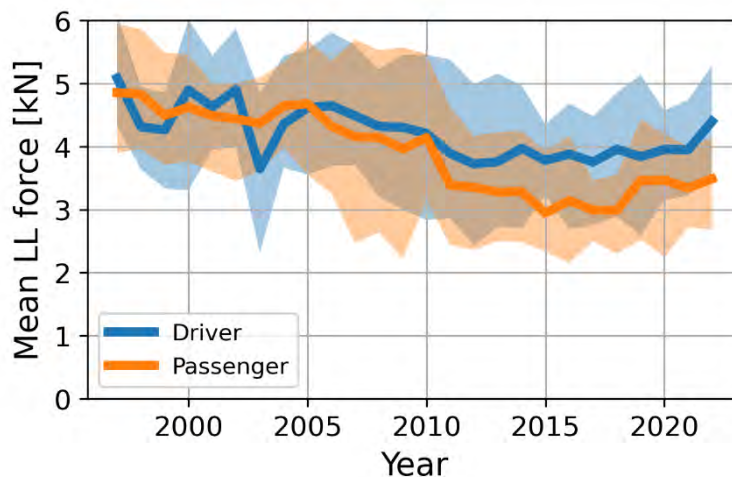


Fig. 9. Mean load-limiter force for devices used at the driver and front-seat passenger positions. The shadowed area shows the range between the 10<sup>th</sup> and 90<sup>th</sup> percentiles of the data observed by year.

Figure 10 shows the adoption of double-stage load-limiter devices and the relation between the forces in the first stage and second stage of the device. Subfigure “a” shows that the adoption of this variation of the load limiter started when the load-limiting devices were present in 80% of the vehicles tested, between 2000 and 2005. Although it was observed a similar adoption for both front-seat occupants, this device was identified in more cases for the driver than for the front-seat passenger between 2010 and 2020. Subfigure “b” shows the relation between the first and second-stage forces observed for the double-stage load-limiter devices. A linear regression was performed, which resulted in a linear function with  $R^2$  equal to 0.495. The result of this regression is shown in the subfigure “b”. Furthermore, quantile regression for the 25<sup>th</sup> and 75<sup>th</sup> quantiles was also performed, showed using the shadowed area. The mean width of this area was 0.66 kN.

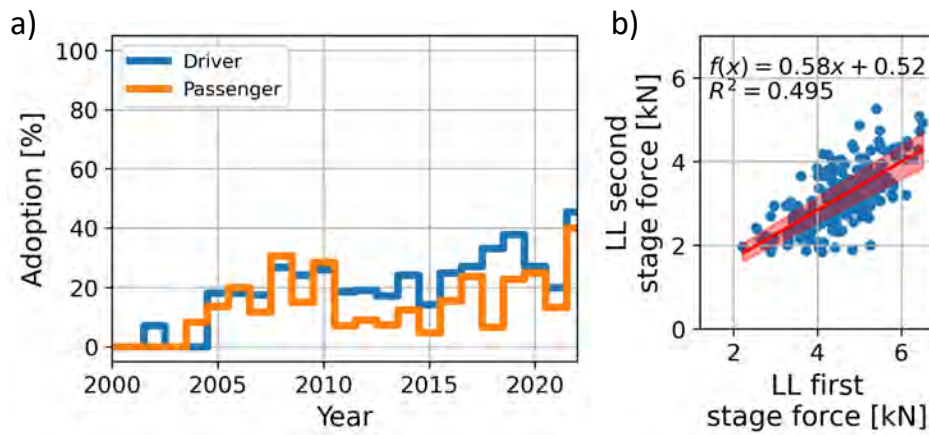


Fig. 10. a) Adoption of double-stage load-limiter devices for the driver and front-seat passenger. b) Relation between the first and second-stage forces observed for the double-stage load-limiter devices. The red line shows the result of a linear regression and the shadowed area shows the 25<sup>th</sup> and 75<sup>th</sup> quantiles.

#### IV. DISCUSSION

As early as 1962, Bertil Aldman stated that “... the occupant must be decelerated in an upright posture. This requires the use of an upper restraint in combination with the lap restraint”. In this work, he performed tests on different safety belt systems in which the three-point seat belt was always more protective than any other restraint tested [15]. The three-point seat belt was first incorporated in a vehicle by Volvo in 1959, and shortly after other carmakers started to install these restraint systems in their vehicles too. The introduction of pre-tensioners in the 1980s and load limiters in the mid-1990s resulted in the seat-belt systems currently present in most vehicles in high-income countries.

Even if all seat belts incorporate these advanced features to optimise the protection of occupants, pre-tensioners and force-limiters can be tuned depending on other vehicle characteristics, such as internal vehicle dimensions, size of the airbags, crashworthiness behaviour, etc., to maximise their effectiveness. Thus, different vehicles will incorporate different pre-tensioning and/or force-limiting values. Even if these devices have been shown to be very effective in reducing the severity of injuries in computational and experimental studies, a more robust assessment of advanced seat belts needs to be done using real-world data [9]. Such evaluation requires knowing which type of pre-tensioner and force limiter was installed in the vehicle, and this information is hardly available in existing real-world collision databases.

This study has applied already-developed algorithms to analyse the time-history seat-belt forces that can be downloaded from NHTSA’s crash database. The algorithms were trained by comparing their predictions with a subset of 3,081 curves from which the values of the peak force and TTF of the pre-tensioner and the stage/s of load limiting had been previously identified by a group of nine people specifically trained to identify these features. To increase the robustness of the method, the authors of the study confirmed the results from the inspection of the curves. Some particular curves that were more difficult to assess were analysed with the help of a seat-belt specialist.

The performance of the algorithm used to identify the presence of pre-tension in a seat belt was extremely high according to the criteria of recall, precision, accuracy and F1-score (95.0%, 89.7%, 95.5% and 92.3%, respectively) used to assess the quality of the predictions. The mean value of the pre-tensioner peak force identified by the algorithm was within 10% of the mean force identified by the trained people who assessed the validation subset. The prediction of load limiting was more challenging, especially in seat belts incorporating a double-stage load limiter which had the lowest F1-score with 0.765.

The data included in the NHTSA crash database match well what has been reported in the literature. Mercedes-Benz introduced pre-tensioners in cars in 1983 [16], as it has also been identified in our analysis. Renault started to install seat belts with a force limiter in 1995. Experts in the field consider force limiters as the most important improvement of the three-point seat belt [17]. The data analysed here showed a few vehicles including a load limiter slightly earlier, but it can also be a limitation of the algorithm. It is interesting to observe that the adoption rate of load limiters has been much faster than in the case of pre-tensioners.

Another relevant consideration is how the peak force of lap-belt pre-tensioners has been increasing steadily

over the last few years while the shoulder-belt pre-tensioner peak force has remained at about the same value since its introduction. The data also show that introducing pre-tensioners in the front seat follows the same trend for the driver and the passenger positions.

It is interesting to realise that the pre-tensioner introduction rate started to increase in the late 1990s, reaching a wide adoption in the mid-2000s. Despite the later development of load limiters compared to pre-tensioners, it was about the same time that they were broadly adopted. This increasing adoption rate could be linked to three events in the late 1990s. First, NHTSA changed from reporting test results in a technical (numerical) format to an easy-to-understand five-star rating system (1994) and began the crash test program for side impacts in NCAP (1997) [18]. Secondly, Insurance Institute for Highway Safety (IIHS) began evaluating frontal crash tests in 1995. Lastly, Euro NCAP released its first results in 1997. Therefore, the desire of car manufacturers to improve the safety ratings of their vehicles could be linked to the following:

- including more conditions in which the vehicles were tested could push for restraint systems with good performance across different crash scenarios;
- the beginning of consumer rating programs to induce improvements in vehicle safety [19];
- introducing a consumer-friendly presentation of the results could allow the consumer to compare the safety performance of different vehicles quickly and easily.

The main limitation of this study is that the seat-belt characteristics are described using only the force-time history curves of the seat-belt forces, without considering other relevant variables that can affect these curves. This limitation applies to the validation subset, manually inspected, and the algorithm's outcome.

The seat-belt characteristics identified in both sets will present some differences with the actual configuration of the pre-tensioner devices used in the vehicles. Factors such as the delay to fire the pre-tensioner device (i.e., difference between the firing command and the actual firing of the device), belt slack, belt geometry, transducer position, and interactions with the airbag and seat affect the measurement of the tension force at the seat-belt. The influence of these factors cannot be quantified using the applied methodology, and therefore they were ignored in the identification of the seat-belt characteristics.

Although the guidelines provided for the manual inspection of the curves (included in the appendix) aimed to restrict the impact of this limitation, the actual configuration of the restraint system will show differences from the values presented in this study, as shown in the example case at the appendix. Furthermore, the aim of this study was to identify if a pre-tensioning force was present in the lap or shoulder belt, but the actual location of the pre-tensioning device in the lap belt could not be identified. Another limitation is that the developed algorithm did not allow to control for the actual duration of the pre-tensioning force, which is something that perhaps can be improved in further improvements of the method.

However, in the absence of any other tool that can provide this information, this study provides a method to obtain approximate values of the seat-belt characteristics that can be later incorporated into real-world data analyses by matching the vehicles' make and model.

The restraint systems identified in this study were updated to a public repository for easy and free access by the research community, which can be accessed through the following link (<https://github.com/Comillas-IIT-MOBIOUS/Seatbelt-characteristics-2023>). These findings can potentially be used to further study how pre-tensioning and load-limiting devices contribute to avoiding injuries and deaths. These studies could either focus on assessing the influence of these devices using real-world data gathered from vehicle crashes or using the distribution of the restraint system parameters to carry out simulations of vehicle crashes.

## V. CONCLUSIONS

A method was developed to identify seat-belt pre-tensioner and load-limiting features by analysing the shape of the force-time history curves measured during a crash test. The method performed well in identifying pre-tensioners and load limiters, although some limitations were observed, such as limited performance with double-stage load limiters. The adoption of pre-tensioners and load limiters began in the mid-1990s, and they were widely adopted after 2005. Little differences were found in the adoption and configuration of these devices for the driver and passenger positions. The study has some limitations, such as the description of complex systems and the limited dataset size. However, it provides insights that could improve the understanding of vehicle manufacturers' advanced restraint system features.

## VI. ACKNOWLEDGEMENTS

The authors would like to acknowledge the students' contribution from the second year of the Master's Degree in Engineering for Mobility and Safety from the Comillas Pontifical University in manually inspecting the force-time history curves. The algorithms to characterise the features of seat-belt systems were developed in Python, using the following libraries: (i) Pre-tensioner characterisation: numpy-ext, binclass-tools; (ii) Time-series clustering: tslearn; (iii) Load limiter characterisation: simplification; (iv) Measure performance metrics: scikit-learn; (v) Storage data: pandas, numpy; (vi) Signal filtering: scipy; (vii) Genetic optimisation: pygad.

## VII. REFERENCES

- [1] National Center for Statistics and Analysis (2022) National Highway Traffic Safety Administration, *Traffic safety facts 2020: A compilation of motor vehicle crash data*.
- [2] Blincoe, L., Miller, T. R., et al. (2023) National Highway Traffic Safety Administration, *The economic and societal impact of motor vehicle crashes, 2019 (Revised)*, Washington, DC.
- [3] AAAM (2016) *Abbreviated injury scale-2015 Revision*.
- [4] Kent, R. W., Crandall, J. R., et al. (2001) SAE Technical Paper, *The influence of superficial soft tissues and restraint condition on thoracic skeletal injury prediction*.
- [5] Kent, R., Forman, J., Parent, D. and Kuppa, S. (2007) Rear seat occupant protection in frontal crashes and its feasibility. *Proceedings of Conference 20th International Conference on the Enhanced Safety of Vehicles*, 2007.
- [6] Forman, J., Michaelson, J., Kent, R., Kuppa, S. and Bostrom, O. (2008) Occupant restraint in the rear seat: ATD responses to standard and pre-tensioning, force-limiting belt restraints. *Proceedings of Conference Annals of Advances in Automotive Medicine/Annual Scientific Conference*, 2008.
- [7] Forman, J., Lopez-Valdes, F., et al. (2009) Rear seat occupant safety: an investigation of a progressive force-limiting, pretensioning 3-point belt system using adult PMHS in frontal sled tests. *Stapp Car Crash Journal*, **53**: p.49.
- [8] Michaelson, J., Forman, J., Kent, R. and Kuppa, S. (2008) Rear seat occupant safety: kinematics and injury of PMHS restrained by a standard 3-point belt in frontal crashes. *Stapp Car Crash Journal*, **52**: p.295.
- [9] Segui-Gomez, M., Lopez-Valdes, F. and Crandall, J. (2009) Characterizing the distribution of injury and injury severity for belted front-seat occupants involved in frontal crashes. *Proceedings of Conference Proceedings of IRCOBI Conference*, 2009, York, UK.
- [10] "Research Testing Databases | NHTSA", <https://www.nhtsa.gov/research-data/research-testing-databases>. [accessed 31/3/2023].
- [11] Ting, K. M., Sammut, C. and Webb, G. I. (2010) Precision and recall. *Encyclopedia of Machine Learning*, Springer, US.
- [12] Sammut, C. and Webb, G. I. (2010) Accuracy. *Encyclopedia of Machine Learning*, Springer, US.
- [13] Sammut, C. and Webb, G. I. (2010) F1-measure. *Encyclopedia of Machine Learning*, Springer, US.
- [14] Visvalingam, M. and Whyatt, J. D. (1993) Line generalisation by repeated elimination of points. *The Cartographic Journal*, **30**(1): pp.46–51.
- [15] Aldman, B. (1962) Biodynamic studies on impact protection. *Acta Physiologica Scandinavica. Supplementum*, **56**(192): pp.1–80.
- [16] Mitzkus, J. E. and Eyrainer, H. (1984) Three-point belt improvements for increased occupant protection. *SAE Transactions*, **93**: pp.1056–1064.
- [17] Håland, Y. (2006) The evolution of the three-point seat belt from yesterday to tomorrow. *Proceedings of Conference Proceedings of IRCOBI Conference*, 2006, Madrid, Spain.
- [18] Hershman, L. I. (2001) The US New car assessment program (NCAP): past, present and future. *Proceedings: International Technical Conference on the Enhanced Safety of Vehicles*, **2001**: p.13.
- [19] Samaha, R. R., Digges, K., Fesich, T. and Authaler, M. (2011) Frontal crash testing and vehicle safety designs: A historical perspective based on crash test studies. Active Safety and the Mobility Industry.

VIII. APPENDIX

**Guideline to identify the pre-tensioner configuration**

Some force-time history curves were used to exemplify how to identify the pre-tensioner configuration. The following figure shows two force-time history curves, one with a pre-tensioning device and the other without.

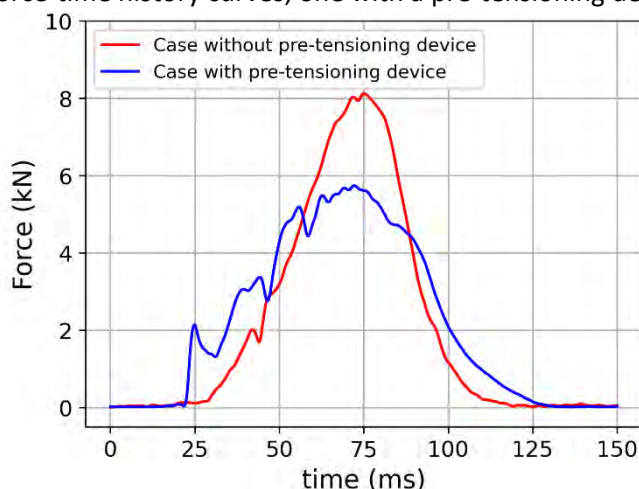


Fig. A11. Force-time history curves for two crash tests. The tension force was measured at the shoulder belt of the driver’s belt. A CFC 180 was applied to both signals.

Two possible scenarios can be observed in Figure A11, the tension force in the belt increased progressively (i.e., a restraint system without a pre-tensioning device in red), and the tension force increased suddenly (i.e., a restraint system with a pre-tensioning device in blue). Figure. A12 “a” shows a zoom-in of the force-time history curves shown above, where only the first 30 ms of the crash can be observed. As can be seen in the figure, there is no sudden increase in the tension force in the case without a pre-tensioning device (red curve). Figure. A12 “b” shows only the case with a pre-tensioning device and the characteristics that were identified in the force-time history curve. The “TTF identified” shows the time-to-fire that was asked to be identified, which is the time at which the tension force begins the sudden increase. The “actual TTF” (i.e., the firing command) would be earlier compared to the “TTF identified”, and it is not influenced by the pre-tensioner delay, belt slack, belt geometry, and transducer position. However, it is not possible to identify this with the available information. The “PP force” is the force of the pre-tensioning device, and it was identified as the first peak after the “TTF identified” using the filtered signal.

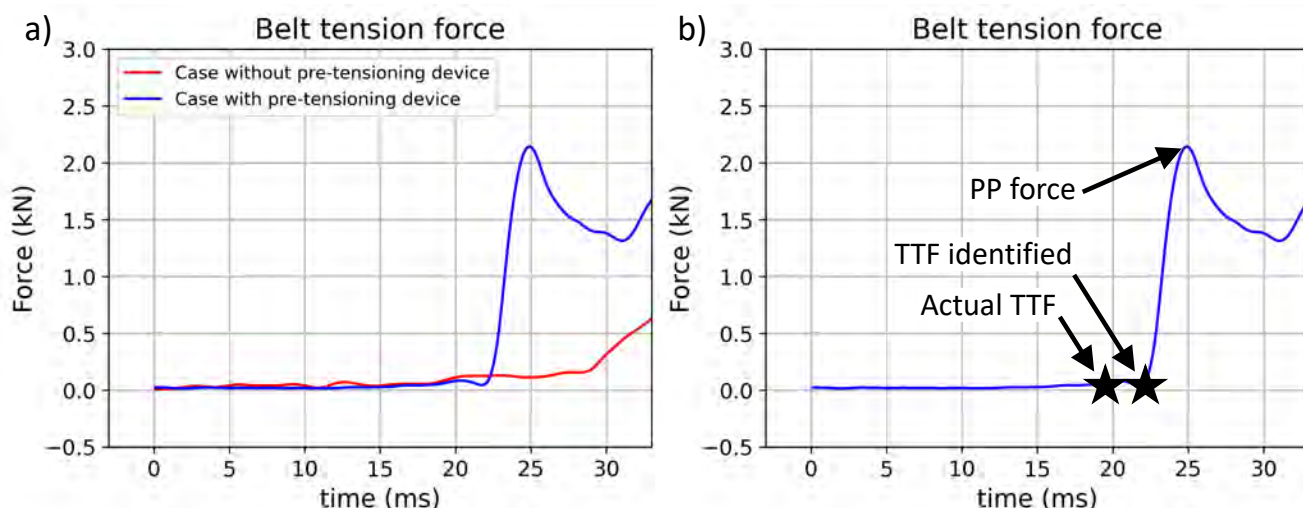


Fig. A12. a) Force-time history curves for two crash tests (same as in Figure A11), only the first 30 ms. The tension force was measured at the shoulder belt of the driver’s belt. A CFC 180 was applied to both signals. b) Force-time history curve of a case with a pre-tensioning device and the characteristics to be identified of the restraint system.

Some cases showed an increase in the shoulder and lap belt, as shown in Figure A13. Case number 1, shown in blue, is the same as the shown in blue in Figure A11 and Figure A12. The other curves, in red, shows a case with pre-tensioning in the lap and shoulder belt. The force-time history curves measured at the lap belt are shown with a dashed line.

The case with a shoulder belt pre-tensioner (in blue) showed a transference of the tension force through the buckle from the shoulder belt to the lap belt. However, the peak in the lap belt tension force can hardly be identified as the result of the pre-tensioning device in the buckle or the anchor plate, as the slope of the force-time history curve is not as high as in cases with a pre-tensioning device. However, the case with a shoulder and lap belt pre-tensioners (in red) showed peaks in both seat-belt sections. These pre-tensioner devices were fired at different times as the shoulder belt tension force increased first. Furthermore, the force-time history curve of the lap belt showed two different slopes. Firstly, a low slope was associated with a transference of the tension force through the buckle, similar to first case in blue, which had a similar slope. Secondly, a high slope which was associated with a pre-tensioning device had a similar slope as the one associated with pre-tensioning devices in the shoulder belt force-time history curves.

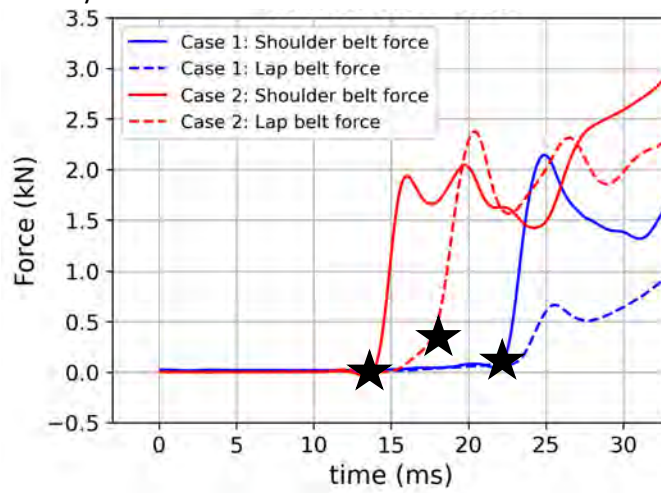


Fig. A13. Force-time history curves for two crash tests, only first 30 ms. The tension force was measured at the shoulder belt (solid line) and lap belt (dashed line) of the driver’s belt. A CFC 180 was applied to both signals. The stars show the time at which the TTF was identified.

**Guideline to identify the load-limiting configuration**

Some force-time history curves were used to exemplify how to identify the load-limiting configuration. For this task, it was gathered cases without load limiting or with load-limiting devices of one and two stages.

The following figure shows three force-time history curves where no load limiting was observed. These force-time history curves showed a range of peak tension force between 5 and 10 kN. However, none of the force-time history curves indicated a sustained tension force over time.

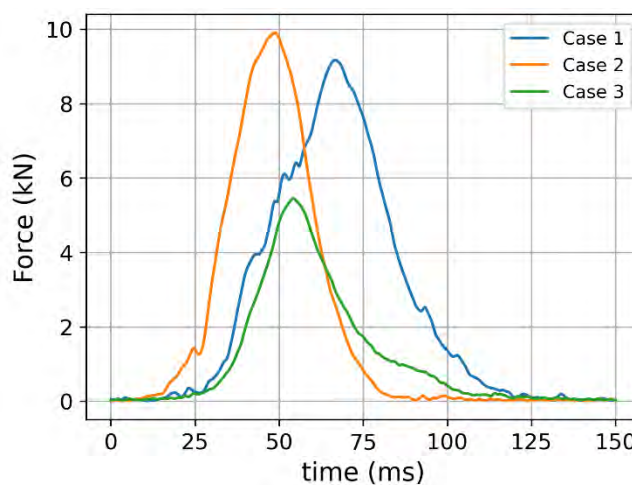


Fig. A14. Force-time history curves for three crash tests. The tension force was measured at the shoulder belt of the driver’s belt. A CFC 180 was applied to all signals.

Figure A15 shows six force-time history curves where a load-limiting device was identified. Some of these force-time history curves were identified as those with a load-limiting device of one stage and others with two. Subfigure “a” shows three force-time history curves where a one-stage load-limiting device was identified. Subfigure “b” shows three force-time history curves where a double-stage load-limiting device was identified.

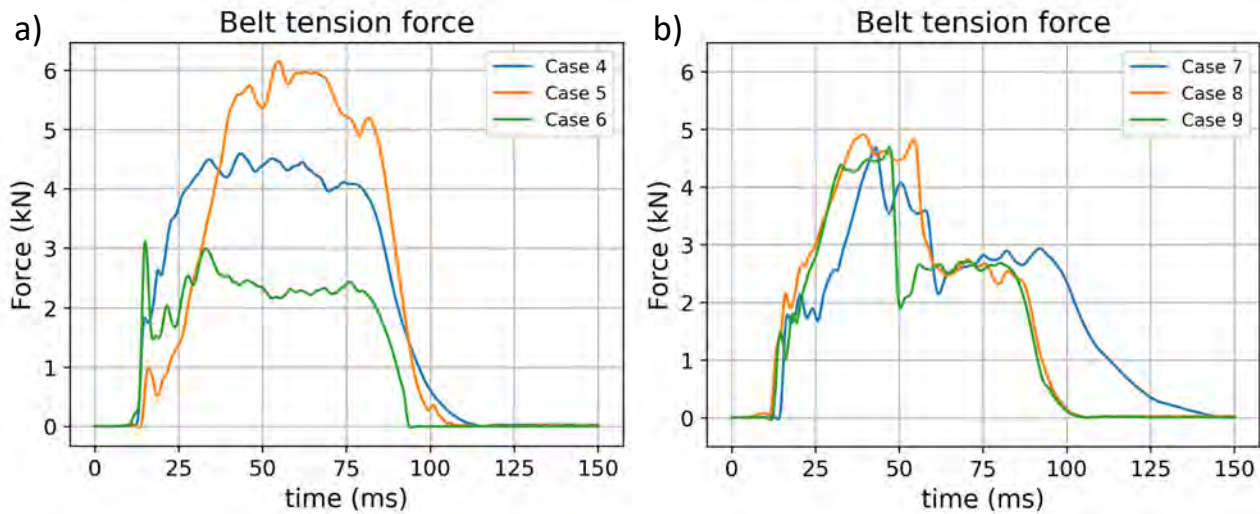


Fig. A15. Force-time history curves for six crash tests. The tension force was measured at the shoulder belt of the driver’s belt. A CFC 180 was applied to all signals. a) Case 4, 5, and 6 with a one-stage load-limiting device used. b) Case 7, 8, and 9 with a double-stage load-limiting device used.

The load-limiting force of the device was identified as the mean force of the stage. This mean was obtained visually and one decimal precision was asked for its identification. Figure A16 shows some examples of how the mean force of the stage was identified.

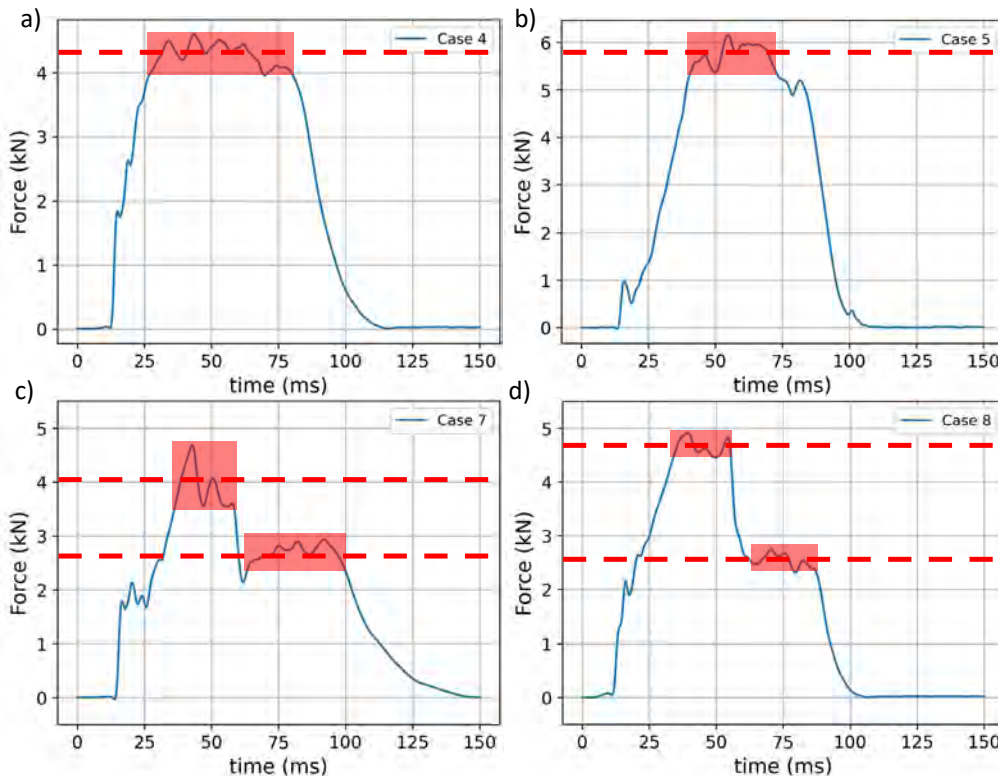


Fig. A16. Force-time history curves for four crash tests. The tension force was measured at the shoulder belt of the driver’s belt. A CFC 180 was applied to all signals. The mean load-limiting force is shown with a red dashed line and each stage of the load-limiting device is shown with a red shadowed square. a) Case 4 with a one-stage load-limiting device used. b) Case 5 with a one-stage load-limiting device used. c) Case 7 with a double-stage load-limiting device used. d) Case 8 with a double-stage load-limiting device used.

Subfigure “a” shows case 4 from Figure A15, this restraint system was identified as one with a one-stage load-limiting device. The stage of the load limiter is shown in red and the mean value of the load-limiting force is shown with a dashed line. Subfigure “b” shows case 5 from Figure A15, this restraint system was also identified as one with a one-stage load-limiting device. Subfigure “c” shows case 7 from Figure A15, this restraint system was identified as one with a double-stage load-limiting device. However, this case also shows load-limiting stages with a slope in the load-limiting force. The first stage of the load-limiting device showed a negative slope, which resulted in a decreasing load-limiting force. The second stage of the load-limiting device showed a positive slope, which resulted in an increasing load-limiting force. Subfigure “d” shows case 8 from Figure A15, this restraint system was also identified as one with a double-stage load-limiting device.

**Examples of seat belt pre-tensioner and load limiter characteristics**

The following figure and tables contain an example of the application of the identification algorithm, the manual identification, and the actual pre-tensioner and load limiter characteristics provided by the seat-belt manufacturer. A similar restraint system configuration was used in the following study: Östling M., Eriksson, L., Dahlgren M., Forman J. (2023) Frontal Head-On Car-To-Heavy Goods Vehicle Crashes Effect on the Restraint System. 27<sup>th</sup> ESV Conference Proceedings, 2023, Yokohama, Japan. Paper Number 23-0198.

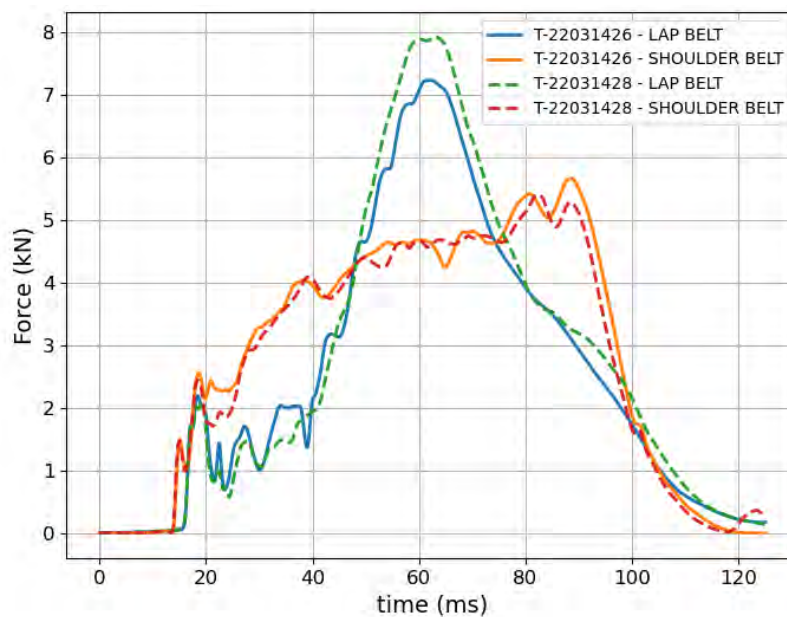


Fig. A17. Force-time history curves for the ‘T-22031426’ and ‘T-22031428’ crash tests. The tension force was measured at the shoulder and lap belt of the occupant. A CFC 180 was applied to all signals.

TABLE II

SEAT-BELT PRE-TENSIONER AND LOAD LIMITER CHARACTERISTICS - LAP BELT - TEST T-22031426

Source	Pre-tensioner force [kN]	Pre-tensioner TTF [ms]	Load limiting force [kN]
Manufacturer	2	15	-
Manual identification	2.1	16	-
Application of identification algorithm	1.8	17	-

TABLE III

SEAT-BELT PRE-TENSIONER AND LOAD LIMITER CHARACTERISTICS - SHOULDER BELT - TEST T-22031426

Source	Pre-tensioner force [kN]	Pre-tensioner TTF [ms]	Load limiting force [kN]
Manufacturer	2	10	4
Manual identification	2.5	13	4.5
Application of identification algorithm	2.1	14.8	4.6

TABLE II

## SEAT-BELT PRE-TENSIONER AND LOAD LIMITER CHARACTERISTICS - LAP BELT - TEST T- 22031428

Source	Pre-tensioner force [kN]	Pre-tensioner TTF [ms]	Load limiting force [kN]
<i>Manufacturer</i>	2	15	-
<i>Manual identification</i>	2	16	-
<i>Application of identification algorithm</i>	1.8	17	-

TABLE III

## SEAT-BELT PRE-TENSIONER AND LOAD LIMITER CHARACTERISTICS - SHOULDER BELT - TEST T- 22031428

Source	Pre-tensioner force [kN]	Pre-tensioner TTF [ms]	Load limiting force [kN]
<i>Manufacturer</i>	2	10	4
<i>Manual identification</i>	2.5	13	4.5
<i>Application of identification algorithm</i>	2.0	14.7	4.6